

Original article

# Synthesis of phenanthridinium–bis-nucleobase conjugates, interactions with poly U, nucleotides and in vitro antitumour activity of mono- and bis-nucleobase conjugates

L.-M. Tumir<sup>a</sup>, I. Piantanida<sup>a,\*</sup>, M. Žinić<sup>a</sup>, I. Juranović Cindrić<sup>b</sup>, Z. Meić<sup>b</sup>, M. Kralj<sup>c</sup>, S. Tomić<sup>d</sup>

<sup>a</sup>Laboratory of Supramolecular and Nucleoside Chemistry, Division of Organic Chemistry and Biochemistry, Ruđer Bošković Institute, Bijenicka 54, HR 10002 Zagreb, P.O.B. 180, Croatia

<sup>b</sup>Laboratory of Analytical Chemistry, Department of Chemistry, Faculty of Science, Horvatovac 102a, HR 10000 Zagreb, Croatia

<sup>c</sup>Laboratory of Functional Genomics, Division of Molecular Medicine, Ruđer Bošković Institute, P.O.Box 180, HR-10002 Zagreb, Croatia

<sup>d</sup>Laboratory for Chemical and Biological Crystallography, Division of Physical Chemistry, Ruđer Bošković Institute, HR 10002 Zagreb, P.O.B. 180, Croatia

Received in revised form 25 April 2006; accepted 4 May 2006

Available online 21 June 2006

## Abstract

Novel bis-nucleobase–phenanthridinium conjugates were synthesised and their aqueous solutions spectroscopically characterised. Bis-adenine conjugate revealed in aqueous solutions significantly more pronounced intramolecular aromatic stacking interactions than bis-uracil analogue. In contrast with previously reported poly A recognition by bis-uracil conjugate, recognition of complementary nucleotides and poly U was not observed due to the strong interference of bulk water with hydrogen bonding between nucleobases. The screening of anticancer activity on six human cell lines revealed that tethering of a nucleobase to phenanthridinium moiety diminished antiproliferative potential of phenanthridinium. However, among mono-nucleobase conjugates adenine derivative was found to be the most selective one (MiaPaCa–2, Hep–2).

© 2006 Elsevier Masson SAS. All rights reserved.

**Keywords:** Phenanthridinium–bis-nucleobase conjugates; Nucleotides; Polynucleotides; In vitro antitumour activity

## 1. Introduction

It is well known that non-covalent interactions between DNA/RNA and peptides or smaller molecules are essential for all processes in living cells. Both types of polynucleotides exhibit a wide range of structural topologies, among which different single stranded (ss-) sequences are quite numerous. While ss-sequences are a ubiquitous part of the RNA folding landscape, there are fewer observations of stable ss-DNA cases, e.g. hairpins [1] and abasic sites [2], to name some of them. Since ds-DNA is protected from reaction with a number of chemical and biological nucleases (see reference [3] and the references therein), some studies have been aimed at exploiting the vulnerable ss-DNA, e.g. hairpin loop regions [4–6]. Furthermore, many of the antitumour drugs act by forming abasic sites in DNA [7]. Since DNA lesions and strand breaks

are also susceptible to the influence of ligand binding with consequences for recognition by repair enzymes, a number of small molecules were synthesised that bind specifically at such lesions with an idea to inhibit the DNA repair system and in that way pronounce the action of antitumour drugs [8]. Most of studied molecules incorporated three structural units: (a) an intercalator unit for strong binding to DNA, (b) a nucleic base for recognition of the complementary non-paired base at the abasic site, and (c) a linker connecting the intercalator and the base of a suitable length and flexibility to enable pairing of a tethered base with that at the abasic site. Linkers of many such intercalator–nucleobase conjugates actively contributed in binding to DNA and under some experimental conditions exhibited also strand cleavage [8]. In previous research we have prepared a series of phenanthridinium–nucleobase conjugates (Scheme 1), characterised by short aliphatic linkers inert toward DNA/RNA, that have shown intriguingly different specificity of binding to ss-polynucleotides [9–11]. Inspired by observed selectivity we have studied interactions of novel phenanthridi-

\* Corresponding author. Tel.: +385 1 45 71 210; fax: +385 1 46 80 195.

E-mail address: [pianta@irb.hr](mailto:pianta@irb.hr) (I. Piantanida).



Scheme 1. Previously studied protonated (4–8) [9,10] and methylated (9–11) [11] phenanthridinium–nucleobase conjugates.

nium–bis-nucleobase conjugates presented in Fig. 1 with DNA and RNA, among which bis-uracil derivative (2) has shown strong selectivity toward homo polynucleotides containing consecutive adenines [12]. Here are presented syntheses of phenanthridinium–bis-nucleobase conjugates, detailed spectroscopic properties in aqueous solution, interactions with nucleotides and poly U and comparable *in vitro* biological activity on six human cell lines of all till now prepared phenanthridinium mono- and bis-nucleobase conjugates (Fig. 1 and Scheme 1).

Newly synthesised compounds 1–3 also introduce two major differences compared to previously studied 4–11: a) an additional nucleobase offers a possibility of doubled recognition between conjugate and complementary polynucleotide [13], b) two linker–nucleobase units tethered to the opposite sites on the longer axis of phenanthridinium result in significantly restricted possibility of phenanthridinium intercalation into polynucleotide. Considering the case b), steric restriction in non-covalent complex formation has already in some cases resulted in strong ss- over ds-polynucleotide preferential binding [14, 15]. Also, intercalative binding mode significantly differentiates between ss- polynucleotides and ds-polynucleotides by means of “neighbour exclusion principle” valid only for latter polynucleotides [16]. Therefore, in this work we present synthesis of compounds 1–3, detailed spectroscopic analysis of intramolecular interactions of bis-nucleobase conjugates 2, 3

combined with molecular modelling and interactions with nucleotides and single stranded uracil polynucleotide. Here presented *in vitro* screening of the antiproliferative activity of phenanthridinium–mono- and bis-nucleobase conjugates (2, 3, 5–8) addressed the impact of tethered nucleobases on the bioactivity of typically DNA intercalative phenanthridinium moiety (1,4).

## 2. Chemistry

### 2.1. Synthesis

The general strategy used for the synthesis of the novel phenanthridine–bis-nucleobase conjugates 1–3 comprises the alkylation of the amino substituents of phenanthridine by dibromopropane, followed by the introduction of nucleobase at the other end of alkyl linker. Novel compound 1, as well as previously known Ade-C<sub>3</sub> (9-(*n*-propyl)adenine) and Ura-C<sub>3</sub> (1-(*n*-propyl)uracil) [17] were prepared for comparison purposes.

As outlined in Scheme 2, 3,8-bis-tosylamino-6-methylphenanthridine was alkylated in the presence of potassium carbonate in dry DMF due to a low solubility in other solvents, e.g. acetonitril. Only the addition of excess of mono- or dibromoalkane afforded bis-alkylated phenanthridines 12 and 13 in acceptable yields (30% and 55%, respectively). For preparation of 12, a large excess of dibromoalkane was essential in order to prevent formation of undesired alkyl-bis-phenanthridine. Again, the large excess of adenine or uracil in reaction with 12 was necessary to obtain compounds 14 and 15 in yields of 34 and 84%, respectively. Under these conditions (Scheme 2) the alkylation of uracil selectively occurred at the N1 position giving 14 as main product but precise temperature control in reaction ( $T = 40\text{--}50\text{ }^{\circ}\text{C}$ ) should be stressed since at higher temperatures 1,3-*N* alkylated uracil became dominant while at room temperature reaction was unreasonably slow (few weeks). Removal of tosyl from 13–15 was achieved by heating at 100 °C in acidic conditions (Scheme 2) and giving compounds 1–3 in 40–93% yields. They were found to be sufficiently soluble in water at acidic conditions, which enabled studies in aqueous media.

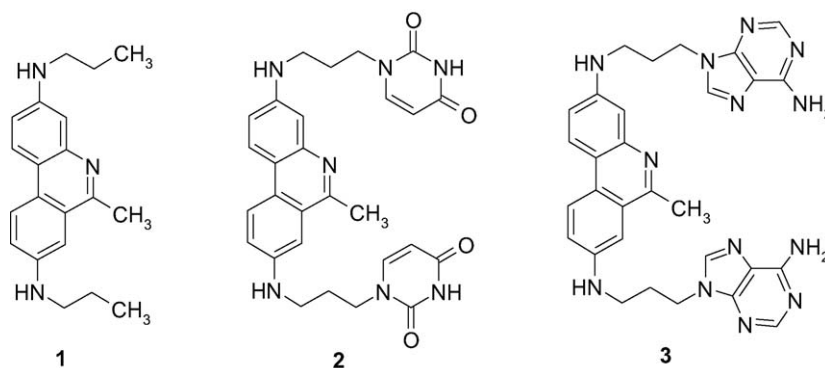
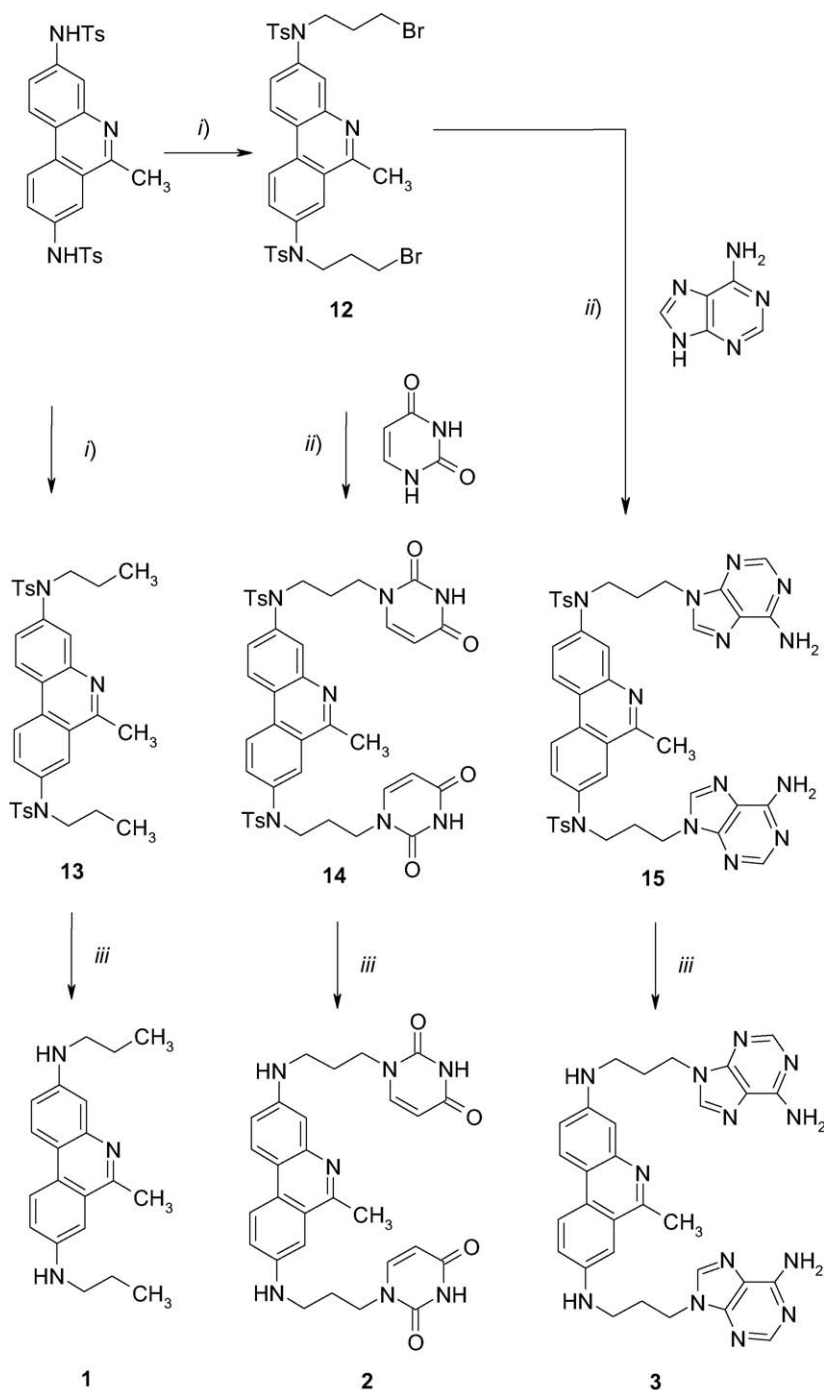


Fig. 1. General structure of novel phenanthridine–bis-nucleobase conjugates.



Scheme 2. i)  $\text{Br}(\text{CH}_2)_3\text{Br}$  or  $\text{Br}(\text{CH}_2)_2\text{CH}_3$ ,  $\text{K}_2\text{CO}_3$ , dry DMF, Ar, r.t., ii) NaH, dry DMF, Ar, 40–50 °C, iii) a) 2:1  $\text{CH}_3\text{COOH}:\text{H}_2\text{SO}_4$ , 80–100 °C, b)  $\text{NaOH}/\text{H}_2\text{O}$ .

## 2.2. Spectroscopic properties

### 2.2.1. UV–vis and fluorescence spectra

UV–vis spectra of aqueous solutions of **1–3** are strongly pH dependent, exhibiting a one step change at  $\text{pK}_a \approx 6$ , attributed to protonation of phenanthridine nitrogen [9]. Due to the low solubility of phenanthridine at pH 7, all further experiments in aqueous media were done at pH = 5, all of compounds being in a protonated (phenanthridinium) form. The UV–vis spectra of compounds **1–3** (at pH = 5, sodium citrate–HCl buffer,  $I = 0.027 \text{ mol dm}^{-3}$ ) obey Lambert–Beer law in the concentra-

tion range of  $5 \times 10^{-6}$ – $8 \times 10^{-5} \text{ mol dm}^{-3}$ . By controlling UV–vis experiments it was observed that aqueous solutions of **1–3** were stable for a few months. In all, hypochromic effect was observed at higher concentrations pointing the presence of intermolecular interactions.

The UV–vis spectrum of bis-adenine conjugate (**3**), if compared with the referent **1**, revealed a pronounced hypochromic effect and bathochromic shift at the one of absorption maximum of phenanthridinium moiety (Table 1,  $\lambda = 287$ – $290$  and  $466$ – $494 \text{ nm}$ ; Fig. 2). An additional maximum in the UV–vis spectrum of **3** at  $267 \text{ nm}$  can be attributed to covalently linked

Table 1  
Electronic absorption data of **1**, **2**, **3** and reference compounds <sup>a</sup>

	$\lambda_{\text{max}} / \text{nm}$ ( $\epsilon / \text{cm}^2 \text{mmol}^{-1}$ )	Hypochromicity (Phen) <sup>c</sup>
<b>1</b>	49500 (287, $\lambda_{\text{max}}$ ); 6000 (466, $\lambda_{\text{max}}$ )	
<b>2</b>	58501 (289, $\lambda_{\text{max}}$ ); 57949 (287 nm); 6900 (485, $\lambda_{\text{max}}$ )	≈ 8% hyperchromicity (287 nm)
<b>3</b>	25011 (267 nm, $\lambda_{\text{max}}$ ); 32810 (290 nm, $\lambda_{\text{max}}$ ); 31995 (287 nm); 4500 (494 nm, $\lambda_{\text{max}}$ )	≈ 38% hypochromicity (287 nm)
Ura-C <sub>3</sub> <sup>b</sup>	9280 (261 nm, $\lambda_{\text{max}}$ ) 2104 (287 nm)	
Ade-C <sub>3</sub> <sup>b</sup>	12871 (261 nm, $\lambda_{\text{max}}$ ) 923 (287 nm)	

<sup>a</sup> Sodium citrate-HCl buffer,  $I = 0.027 \text{ mol dm}^{-3}$ , pH = 5.

<sup>b</sup> Sodium cacodilate-HCl buffer,  $I = 0.05 \text{ mol dm}^{-3}$ , pH = 5 [9].

<sup>c</sup>  $\{[\epsilon_{287 \text{ nm}}(\mathbf{1}) + 2 \times \epsilon_{287 \text{ nm}}(\text{Ura-C}_3 \text{ or Ade-C}_3)] - \epsilon_{287 \text{ nm}}(\mathbf{2} \text{ or } \mathbf{3})\} / [\epsilon_{287 \text{ nm}}(\mathbf{1}) + 2 \times \epsilon_{287 \text{ nm}}(\text{Ura-C}_3 \text{ or Ade-C}_3)] \times 100$ .

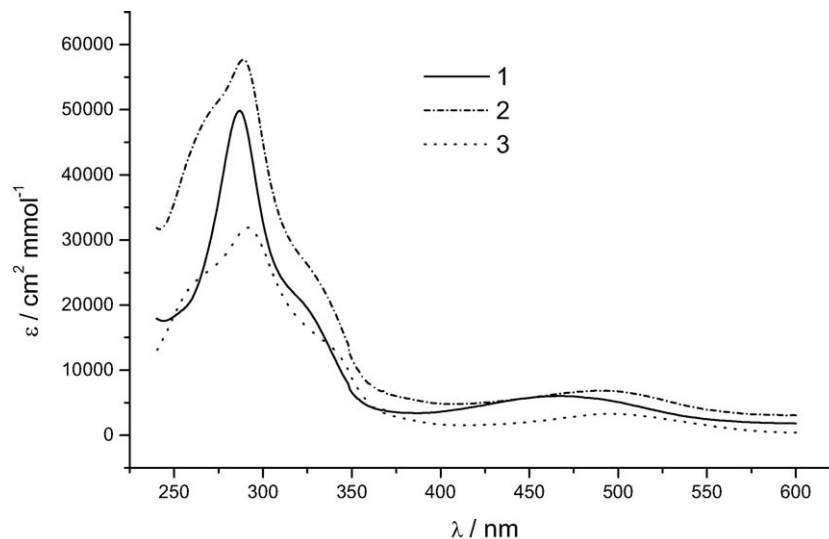


Fig. 2. UV-vis spectra of **1**, **2**, **3** (at pH = 5, sodium citrate-HCl buffer,  $I = 0.027 \text{ mol dm}^{-3}$ ).

adenines since it agrees well with the maximum of the referent adenine analogue Ade-C3 [9] (Table 1,  $\lambda = 262 \text{ nm}$ ). Under assumption of ideal additivity of chromophores in **3** (phenanthridinium, two adenines), the calculated hypochromic effect at 287 nm (38%, Table 1) is quite significant. All effects observed for **3** point toward intramolecular a stacking interactions between phenanthridinium and covalently linked adenines.

UV-vis spectrum of bis-uracil conjugate **2** does not reveal any obvious hypochromic effect if compared with that of **1** but clearly shows bathochromic shift of phenanthridinium maximum (Table 1,  $\lambda =$  from 287 to 289 and  $\lambda =$  from 466 to 485 nm; Fig. 3). Even under presumption of ideal additivity of chromophores in **2** (phenanthridinium, two uracils), hypochromic effect was not evident (Table 1). A new shoulder at about 270 nm in the spectrum of **2** corresponds well to the maximum of the referent uracil analogue Ura-C3 [9] (Table 1,  $\lambda = 268 \text{ nm}$ ) and therefore can be attributed to covalently linked uracils.

UV-vis spectrum of aqueous solution of **3** has shown strong temperature dependence (Fig. 3). In the temperature range between 25 and 60 °C (Fig. 3a) the absorbance maximum at  $\lambda = 267 \text{ nm}$  (attributed to adenines of **3**) was increasing and the maximum attributed to the phenanthridinium of **3** was decreasing and shifting to longer wavelengths ( $\lambda =$  from 290 to

294 nm). A further temperature increase (Fig. 3b) yielded roughly proportional increase of the complete spectrum. Upon cooling to 25 °C the starting spectrum was not completely recovered. In the same temperature range (25–90 °C) UV-vis spectra of **1** and **2** do not change.

The increase of absorbance at  $\lambda = 267 \text{ nm}$  in the spectrum of **3** upon temperature raise is consistent with a breaking (dissociation) of aromatic stacking interactions of adenines and phenanthridinium. However, a peculiar decrease of absorbance at about 290 nm in 25–60 °C temperature range and bathochromic shift suggested even more efficient aromatic stacking interactions of phenanthridinium. Since, according to the isosbestic point at  $\lambda = 270 \text{ nm}$ , only two species are in equilibrium it seems reasonable to propose unstacking of one adenine (absorbance increase at 267 nm) followed by formation of a second adenine-phenanthridinium complex characterised by its UV-vis spectrum with even more pronounced hypo- and bathochromic effects than observed for two adenines-phenanthridinium complex (dominant at 25 °C). A proportional increase in the complete spectrum of **3** at temperatures higher than 60 °C agrees well with the dissociation of second adenine-phenanthridinium complex. All afore mentioned suggested that at 25 °C both adenines are stacked on the same side of phenanthridinium moiety. Such a structure could explain dissociation

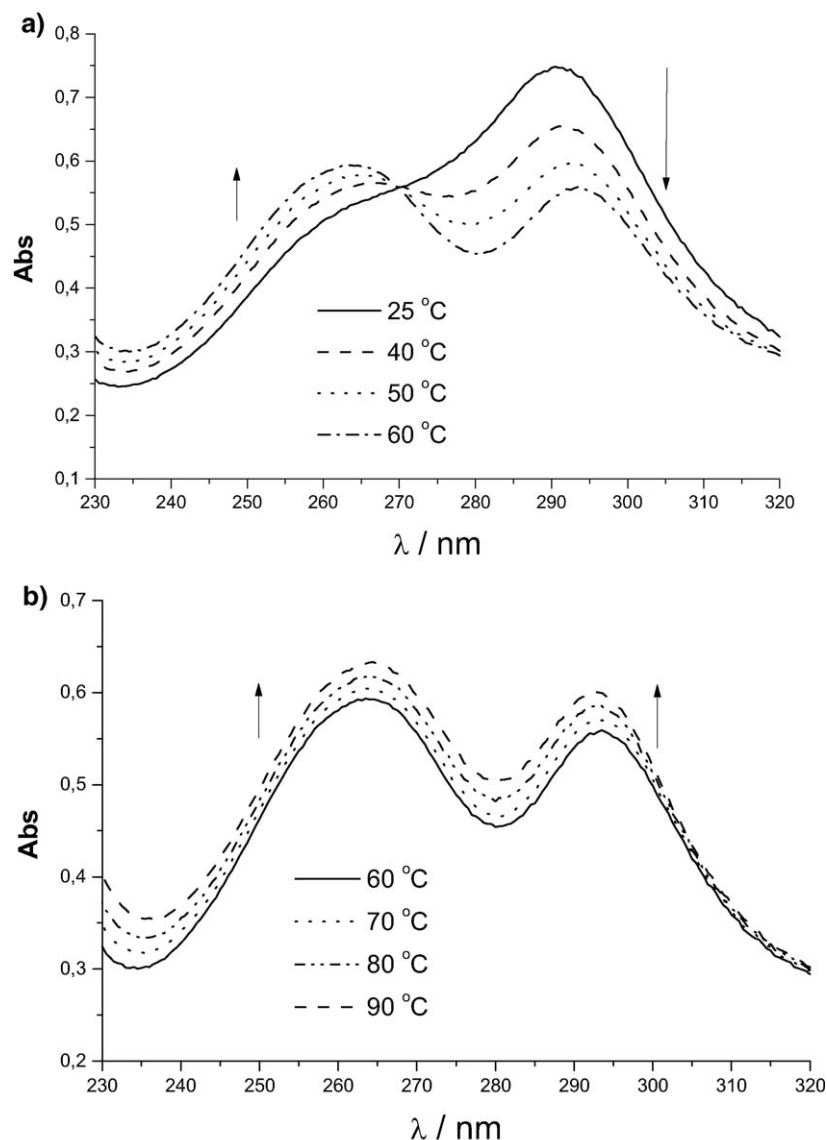


Fig. 3. Temperature dependent changes of UV-vis spectrum of **3** ( $c(\mathbf{3}) = 3.8 \times 10^{-5} \text{ mol dm}^{-3}$  at pH = 5, sodium citrate-HCl buffer,  $I = 0.027 \text{ mol dm}^{-3}$ ): a) 25, 40, 50, 60 °C; b) 60, 70, 80, 90 °C.

of one adenine in the range 25–60 °C followed by a more efficient stacking of the remaining adenine thus causing effects presented on Fig. 3a.

All studied compounds (**1–3**) in aqueous solutions exhibit fluorescence emission linearly dependent on the compound concentration up to  $c = 7.0 \times 10^{-6} \text{ mol dm}^{-3}$ . Excitation spectra monitored at emission maxima of all compounds agree well with the UV-vis spectra. Significantly higher fluorescence emissions of compounds **2** and **3** compared with the reference

compound **1** (Table 2) support intramolecular aromatic stacking interactions between phenanthridinium and linked nucleobases. Quenching of **2** and **3** fluorescence upon temperature increase, while virtually no change in the emission spectra of **1** being observed, was consistent with the unstacking of intramolecular complexes of **2** and **3** [9,11].

Hypochromic shift of **2** and **3** emission maximum compared to reference **1** (Table 2) agrees well with the effect observed for most aromatic compounds upon intercalation into DNA [18], pointing also toward intramolecular stacking interactions.

#### 2.2.2. NMR experiments in aqueous solutions

$^1\text{H}$  NMR spectra of compounds **1**, **2** and **3** were recorded at 600 MHz in water solutions (sodium cacodylate in  $\text{D}_2\text{O}$ -DCl buffer,  $I = 0.005 \text{ mol dm}^{-3}$ , pD = 5, water signal suppressed using pre-saturation technique). Chemical shifts ( $\delta/\text{ppm}$ ) of aromatic protons of **1** and **2** were found to be concentration

Table 2

Fluorescence emission and excitation properties of **1–3** in aqueous solutions (at pH = 5, sodium citrate-HCl buffer,  $I = 0.027 \text{ mol dm}^{-3}$ )

	$\lambda_{\text{exc}}$ (nm)	$\lambda_{\text{em}}$ (nm)	$\text{INT}_{\text{compd}}/\text{INT}_{\mathbf{5}}$ <sup>a</sup>
<b>1</b>	285	585	1
<b>2</b>	290	580	1.5
<b>3</b>	290	580	2.7

<sup>a</sup>  $\lambda_{\text{ex}} = 290 \text{ nm}$ .

dependent ( $c = 1.0 \times 10^{-4}$ – $1.0 \times 10^{-3}$  mol dm<sup>-3</sup>) due to self-stacking interactions (estimated  $K_{sa}$  of  $10^2$  mol<sup>-1</sup> dm<sup>3</sup>) [9].

Proton chemical shifts  $\delta_0$  of **1** and **2** were obtained by extrapolation of dependence of  $\delta$  versus concentration to infinite dilution, where no intermolecular self-association was present [19]. Chemical shifts  $\delta_0$  of aromatic protons of **2** were strongly shifted upfield (0.1–0.3 ppm) relative to **1** signals, due to intramolecular aromatic  $\pi \dots \pi$  interactions between phenanthridinium and covalently attached uracil moieties.

Interestingly, using the same experimental conditions, aqueous solution of **3** didn't show any signals in <sup>1</sup>H NMR spectrum. Proton signals could be observed only at probe temperatures higher than 50 °C. Adding DMSO in water solution of **3** caused also appearance of proton signals (volume portion of DMSO more than 30%;  $c(\mathbf{3}) > 1 \times 10^{-4}$  mol dm<sup>-3</sup>). This behaviour can be explained by formation of large aggregates of **3** molecules in water solution, even at unexpectedly low concentration.

### 2.3. Molecular modelling, molecular mechanics, molecular dynamics and semiempirical study performed for **2** and **3**

Molecules **2** and **3** were built in extended (E) and folded S-shape (with the nucleobases stacking phenanthridinium from

Table 3

Results of the semiempirical, AM1 calculations (in vacuum) and of the force field calculations (AMBER, with the effect of the bulky water simulated by the distance dependent dielectric constant)

Compound		AM1	AMBER
<b>2</b>	Conformation	$\Delta E$ (kcal mol <sup>-1</sup> )	$\Delta E$ (kcal mol <sup>-1</sup> )
	E	10.6	12.2
	S	3.6	3.4
	G	2.5	1.4
	G <sub>0</sub>	0.0	0.0
<b>3</b>	Conformation	$\Delta E$ (kcal mol <sup>-1</sup> )	$\Delta E$ (kcal mol <sup>-1</sup> )
	E	4.1	15.9
	S	0.0	0.0
	G	0.4	0.6

different sides of the plane) and G-shape (with nucleobases in stacking interaction with phenanthridinium from the same side of the plane) conformations using the program InsightII [20] (Fig. 4).

#### 2.3.1. Semiempirical MO and MM calculations for **2** and **3**

Quantum mechanical, AM1 calculations were performed in order to determine partial atom charges (to be used for empirical calculations), and relative potential energies of different conformations of **2** and **3** in vacuum.

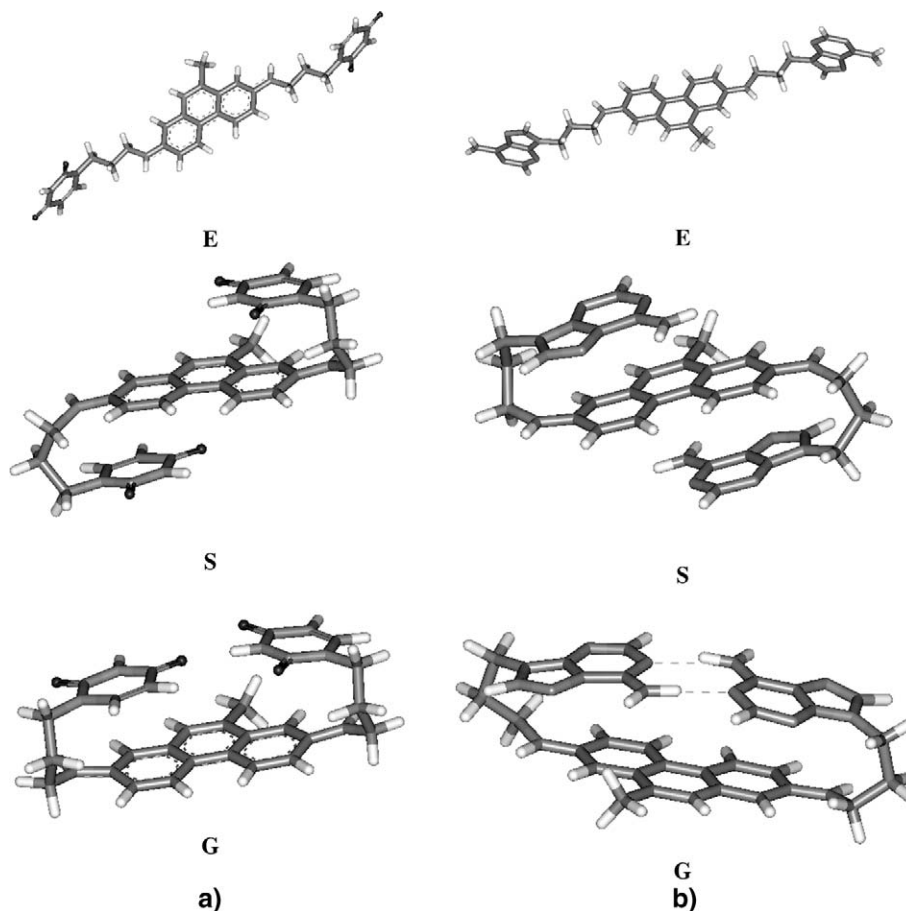


Fig. 4. Optimised structures of different conformations (E, extended, S, with nucleobases stacked on different sides of phenanthridinium plane, G, with nucleobases stacked on the same side of phenanthridinium plane) of compounds **2** (Fig. 4a) and **3** (Fig. 4b).

Molecular modelling of the possible conformations of compounds **2** and **3** in water was accomplished by molecular mechanics (MM) calculations and molecular dynamics (MD) simulations performed with the AMBER force field and the partial charges determined by the semiempirical (AM1) calculations. Two types of calculations were accomplished: a) with the effect of the bulky water simulated by the distance dependent dielectric constant ( $\epsilon = 80r$ ) and, b) using the explicit water molecules. According to the molecular modelling results, both semiempirical and MM, for **2** and **3**, folded G- and S-shape conformations, are more favourable than the extended one (Table 3). The lowest energy conformation  $G_0$  of **2** has three intramolecular H-bonds: two  $O\cdots H-N$  between uracils and the  $O\cdots H-N$  bond between the uracil and phenanthridinium.

The screening of electrostatic interactions slightly changed the relative stability of conformers in such a way that the stacking between nucleobases and phenanthridinium became more pronounced (Fig. 4a). The energy difference between the folded, G-shape and S-shape, and the extended E conformation increased. This is specially pronounced in the case of bis-adenine compound **3** with the S-shape conformation being the most stable. However, the potential energy difference between the S- and G-shape conformers of **3** is small and we expect to have both of them similarly populated in the solution. MD simulations revealed different behaviour of **2** and **3**.

### 2.3.2. MD simulations of **2**

MD simulation of **2** at room temperature (298 K, the effect of the bulky water simulated with the distance dependent dielectric constant) revealed transitions between different conformations. Independently of a starting conformation, (S,  $G_0$  and E were used as initial conformations) the folded conformations,

close to the G-shape, were the most populated. The extended conformation changed to the folded one after only a few tenths of ps. Firstly, folded one of the side chains, and then the other, both on the same side of the phenanthridinium plane. After about 200 ps the molecule folded to so called G-shape conformation and remained as it, with some minor fluctuations, until the end of simulation (Fig. 5), total time of the simulations varied from 0.5–1.5 ns. The S-shape conformation also changed to the G-shape one during the MD simulation and remained in it most of the time. During the MD simulation with the G-shape conformation as an initial one the changes were less significant although transitions to the semi E- and S-shape conformations also occurred.

As a measure of strength of the stacking interactions we considered distance between the centre of the uracil ring and middle of the closer phenyl of the phenanthridinium unit ( $d(X1, XL)$  and  $d(X2, XD)$ ), see Fig. 5). Percentages of conformations sampled during the MD simulation (every 100 fs) that have these distances below 3.5, 4.0, and 4.5 Å are given in Table 4. In the same table given is the distance between two

Table 4

Percentages of distances between the uracil rings and between each uracil and the phenanthridinium unit plane (Fig. 5) sampled during four MD simulations (0.5 ns each). The initial conformation for each simulation is given in the first column on the left

Initial conformation	% $d(X1, X2)$ > 10 Å, 13 Å, 17 Å	% $d(X1, XL)$ < 3.5 Å, 4.0 Å, 4.5 Å	% $d(X2, XD)$ < 3.5 Å, 4.0 Å, 4.5 Å
E	85, 28, 3	18, 58, 70	1, 23, 62
E* <sup>a</sup>	3, 0, 0	29, 81, 96	16, 68, 89
S	13, 1, 0	11, 53, 80	26, 80, 96
G	21, 3, 0	23, 72, 88	23, 72, 89

<sup>a</sup> E\* is continuation of E simulation. Both simulations were running for 0.5 ns.

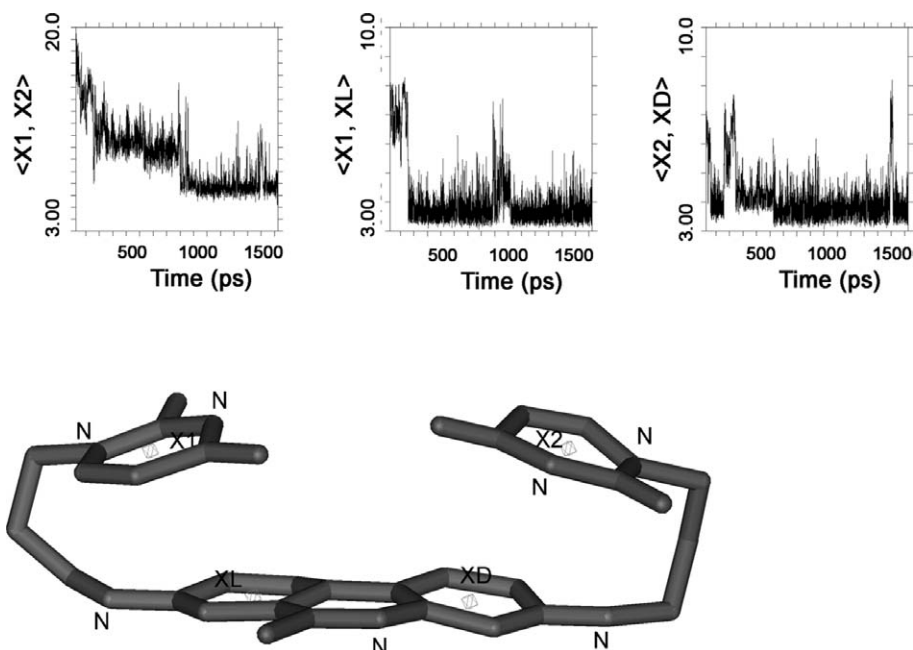


Fig. 5. Conformational changes (distances between aromatic rings) that occurred during the simulation and the final, geometry optimised conformation of **2**. Hydrogens are omitted for simplicity.

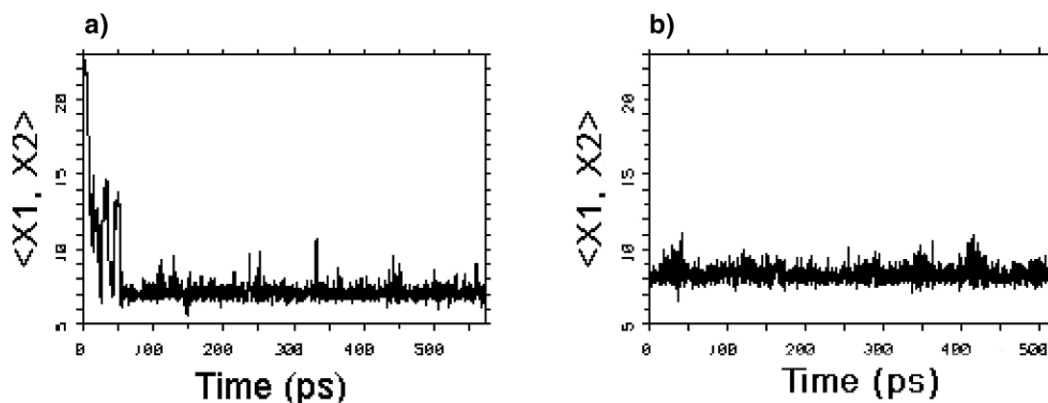


Fig. 6. Conformational changes (distances between adenine rings) that occurred during MD simulation starting from E conformation (Fig. 6a) and S conformation (Fig. 6b) of **3**.

uracil centres,  $d(X1, X2)$ . In the folded, G-shape and S-shape conformations it is slightly below 7 and 9 Å, respectively. A value of this distance between 10 and 13 Å corresponds to partly folded conformation, transition from E to either S or G, with only one nucleobase stacked with phenanthridinium. From the results presented in Table 4 it is apparent that **2** is in solution mostly folded (less than 1% of molecules are in extended form when results of MD simulations started from different conformations are combined).

According to the results of MD we can conclude that influence of water and its possibility to form the hydrogen bond with N1 hydrogen of phenanthridinium favours stacking interactions.

### 2.3.3. MD simulations of **3**

The course of MD simulation for **3** much more depends of the starting conformation than it is observed for **2**. MD simulations with the effect of the bulky water simulated by the distance dependent dielectric constant ( $\epsilon = 80r$ ) at room temperature (298 K) revealed conformational transitions only in the case of E conformation as the starting one (Fig. 6a). In this case, the conformational transition to the folded, G-shape conformation occurred after about 50 ps of simulation at room temperature (Fig. 6a). In the case of S conformation as the starting one, no conformational transition was recorded during the 0.5 ns of simulation at room temperature (Fig. 6b). The mean distance between the geometrical centres of adenines is 7.2 Å in the first case, and 8.4 Å in the second case (the first 50 ps were not used for averaging).

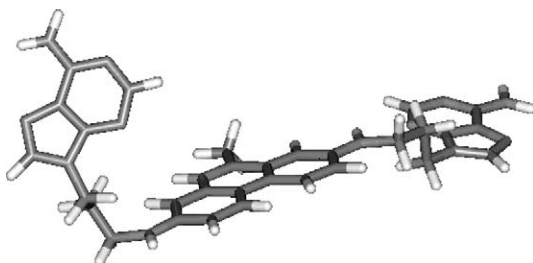


Fig. 7. Conformation of **3** after the MD simulation with explicit water molecules (omitted for clarity) and the mild geometry optimization.

No one of MD simulations with explicit water molecules, starting from different initial conformations, has revealed any conformational transition during the first 200 ps at room temperature. Increasing temperature to 350 K revealed a conformational change from the extended to the folded conformation, after about 400 ps. At the end of 0.5 ns of MD simulation at the increased temperature the molecule is in ‘half S’ conformation (Fig. 7).

Since the molecular dynamic simulations in water were rather short we suspect that influence of the water molecules on solute was not properly investigated. In order to estimate changes in hydrophobic to hydrophilic ratio related to the conformational changes we determined the ratio between polar and non-polar solvent accessible surface area for each conformation of bis-nucleobase conjugates of phenanthridinium (data not given). The ratio is smallest for the extended, and the highest for the folded, S-shape, conformation. This means that ratio between the stabilizing, polar solute – solvent interactions, and the negative influence of water due to its contact with non-polar parts of the molecule is, in agreement to the results of molecular mechanics and dynamics calculations, the highest in the folded, S conformation, the most favourite conformation of **3**.

### 2.4. Interactions of **1–3** with nucleotides

Addition of nucleotides to aqueous solutions of **1–3** didn’t induce any significant changes in their UV–vis spectra, quite similar as noted for previously studied phenanthridinium–nucleobase conjugates [9,11]. Nevertheless, titrations of **1–3** with nucleotides resulted with changes in their fluorescence spectra, quantity of emission change being strongly dependent on a nucleobase covalently attached to phenanthridinium and also on a type of nucleotide added (Table 5). To obtain the binding constants ( $K_s$ ), fluorescence titration data were processed by SPECFIT giving in general the best fit for the 1:1 stoichiometry of complexes (Table 5).

Calculated binding constants ( $K_s$ ) were of the same order of magnitude as those found for ethidium bromide [21,22] and other phenanthridinium–nucleobase conjugates [9,11]. By comparing the fluorescence changes (Table 3,  $\Delta INT$  %) in most cases the tendency  $\Delta INT$  % (**3**) <  $\Delta INT$  % (**2**) <  $\Delta INT$

Table 5  
Binding constants ( $\log K_s$ ) for various 1–3/nucleotide complexes<sup>a,b</sup>

		AMP	GMP	UMP	CMP
<b>1</b>	$\Delta\text{INT}^c$ %	97	68	13	–10
	$\log K_s$	1.63	1.23	< 1 <sup>d</sup>	1.2
<b>2</b>	$\Delta\text{INT}^c$ %	70	49	5.5	–4
	$\log K_s$	1.72	1.02	< 1 <sup>d</sup>	1.38
<b>3</b>	$\Delta\text{INT}^c$ %	25	17	6	–7
	$\log K_s$	1.2	1.27	< 1 <sup>d</sup>	1.2

<sup>a</sup> Fluorimetric titrations were performed at pH = 5 ( $I = 0.027 \text{ mol dm}^{-3}$ , sodium citrate–HCl buffer).

<sup>b</sup> AMP<sup>2-</sup> = adenosine monophosphate; GMP<sup>2-</sup> = guanosine monophosphate; UMP<sup>2-</sup> = uridine monophosphate.

<sup>c</sup>  $\Delta\text{INT}^c$  % =  $[(\text{INT}_0 - \text{INT})/\text{INT}_0] \times 100$ ; INT<sub>0</sub>, relative fluorescence intensity of pure compound, INT, relative fluorescence intensity calculated for 100% of complex formed.

<sup>d</sup> Less than 50% of complexation was reached allowing only estimation of binding constant.

% (**1**) is evident. Since intramolecular stacking interactions have a stronger impact on fluorescence properties of **3** than on **2** it is reasonable to expect that addition of nucleotide will have less influence on the emission of the former. Same explanation agrees well with highest  $\Delta\text{INT}$  % values found for **1** where no intramolecular stacking interactions can exist.

Fluorescence increase of **1–3** solutions upon addition of AMP, GMP and UMP can be explained by mechanism proposed for ethidium bromide and its derivatives having primary or secondary amino groups at 3,8 positions of the phenanthridinium ring [23]. However, unexpected quenching of fluorescence was observed for all studied compounds upon addition of CMP. Up till now, no ethidium bromide derivative is known to exhibit such selectivity for any nucleotide. Actually, small molecules that recognise any nucleotide by opposite spectroscopic changes upon formation of non-covalent complex are extremely rare (e.g. proflavine recognition of GMP [24], bisacridine differentiation between purine and pyrimidine nucleotides [25] and none has shown recognition of only CMP compared to other nucleotides. Therefore, it is not possible to propose explanation of observed quenching of **1–3** solutions upon addition of CMP without detailed photophysical studies which is out of the scope of this publication.

### 2.5. Interactions of 1–3 with polynucleotides

Although **1–3** didn't show any recognition of complementary nucleotides, **2** showed selective interactions within more lipophilic microenvironment of polynucleotides characterised by consecutive adenines [12]. Also, in our previous research analogue of **3** (mono-adenine conjugate) [10] has shown recognition of complementary poly U. Therefore, we have performed detailed studies of **1–3** interactions with single stranded (ss-) polynucleotide poly U. Contrary to previously studied ds-polynucleotides [12], addition of ss-polynucleotide poly U to **1** resulted in fluorescence quenching, while emission of **2** and **3** was first quenched up to the ratio  $r(\mathbf{2}) = 0.05$ ,  $r(\mathbf{3}) = 0.15$  and than strongly enhanced. The observed quenching of fluorescence was quite unexpected (especially for referent **1**) since fluorescence of **EB** was increased by addition of any polynu-

Table 6  
Growth inhibitory effects of different phenanthridinium–nucleobase conjugates **2**, **3** and **5–8** and referent compounds **1** and **4** on the growth of malignant tumour cell lines in comparison with their effects on the growth of normal human diploid fibroblast (WI 38)

	IC <sub>50</sub> (μM) <sup>a</sup>					
	HeLa	MCF-7	MiaPaCa-2	Hep-2	SW 620	WI 38
<b>1</b>	4 ± 0	4 ± 0.4	10 ± 5	7 ± 2	4.4 ± 5	14 ± 14
<b>2</b>	> 100	> 100	≥ 100	> 100	> 100	> 100
<b>3</b>	> 100	> 100	> 100	> 100	> 100	> 100
<b>4</b>	43 ± 18	49 ± 19	> 100	77 ± 40	39 ± 45	≥ 100
<b>5</b>	43 ± 3	44 ± 38	58.5 ± 9	47 ± 38	38 ± 13	> 100
<b>6</b>	> 100	> 100	66 ± 25	42 ± 12	≥ 100	> 100
<b>7</b>	15 ± 10	41 ± 1	50 ± 1	46 ± 6	61 ± 33	88 ± 8
<b>8</b>	84 ± 20	59 ± 18	51 ± 14	57 ± 32	62 ± 24	≥ 100

<sup>a</sup> IC<sub>50</sub>; the concentration that causes a 50% reduction of the cell growth.

cleotide or nucleotide. Another interesting point is that affinity of **1** toward poly U ( $\log K_s = 4.2$ ,  $n = 0.5$ ) is one order of magnitude higher than found for **EB** under same experimental conditions ( $\log K_s \approx 3$ ) [26]. Opposite spectroscopic changes found for **2** and **3** upon titration with poly U point toward existence of at least two different complexes, thus allowing only estimation of stability constants ( $\log K_s < 3$ ) and ratios  $n$  for conditions of high excess of polynucleotide (fluorescence increase). Neither **2** nor **3** (complementary to poly U) didn't show any selectivity toward poly U, pointing toward minor (if any) impact of interactions between nucleobase attached to phenanthridinium with uracil of poly U.

## 3. Pharmacology

### 3.1. Antiproliferative effect of compounds in vitro

The compounds **1–3** and **4–8** were tested for the potential antiproliferative effect on the panel of six human cell lines, five of which are derived from five cancer types: HeLa (cervical carcinoma), MCF-7 (breast carcinoma), SW 620 (colon carcinoma), MiaPaCa-2 (pancreatic carcinoma), Hep-2 (laryngeal carcinoma) and WI 38 (diploid fibroblasts). The compounds showed different antiproliferative effect on the presented panel cell lines (Table 6). The compounds **2** and **3** produced little or no growth inhibition. The compounds **4–8** showed accentuated inhibitory effect on all cell lines, but mostly at the highest tested concentration. Among these compounds **5** and **6** were the most selective ones, since they did not inhibit a growth of normal fibroblasts. On the other side, the compound **1** was the most active one. Besides, the compound **1** was cytotoxic to all cell lines. It should be also taken into consideration that **3**, **4**, **6** and **8** formed colloid DMSO stock solutions used in experiments.

## 4. Conclusions

Spectroscopic methods (UV–vis, fluorescence, NMR) clearly point to the intramolecularly stacked conformation of adenine conjugate **3**. Thermal UV–vis experiments of **3** reveal unstacking of one adenine at up to 60 °C and second adenine at much higher temperatures (Fig. 8). These observations are ad-

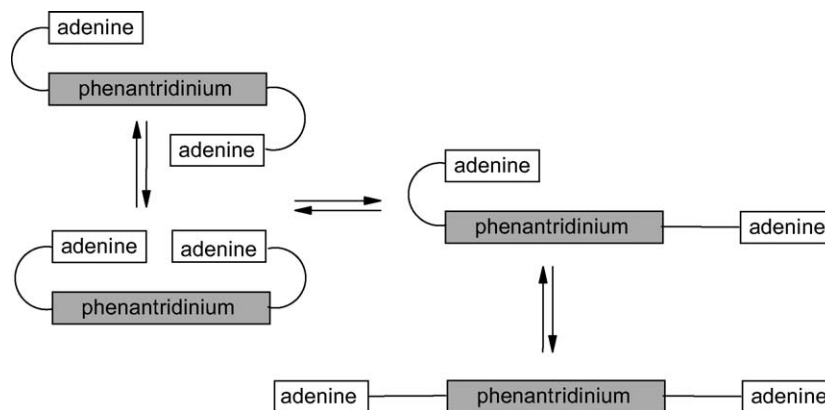


Fig. 8. Schematic representation of possible temperature dependent changes of intramolecular conformation of **3**.

ditionally confirmed by molecular modelling experiments, which showed that the S conformation (with adenines stacked on different sides of the phenanthridinium plane) is the most stable one. However, the potential energy difference between the G-shape and the S-conformers is low (about  $0.6 \text{ kcal mol}^{-1}$ , at the room temperature) and their population in water solution is similar, according to MM and MD results.

Differently, the extended conformation has significantly higher potential energy. The NMR and fluorescence spectra of **2** also revealed the folded conformation of molecule characterised by aromatic stacking interactions between phenanthridinium and covalently linked uracils although the effects are less pronounced than for **3**. Smaller NMR and fluorescence effects of **2** and negligible differences in UV–vis spectrum (compared to referent **1**) suggested much weaker intramolecular interactions between phenanthridinium and uracils than observed for **3**. The molecular modelling revealed frequent transition between different conformations, with the population of fully extended being less than 1%. The G-shape conformation, additionally stabilised by hydrogen bonds between uracil rings, is according to the results of molecular modelling the most stable one, but the energy difference between this and extended conformation is lower than in the case of **3**. Weaker intramolecular stacking interactions in **2** than in **3**, same as observed for previously examined compounds **5–8**, **10–11** [9,11], also agreed well with the finding that large condensed aromatics in water bound more strongly purine than pyrimidine nucleosides and nucleotides [21].

The lack of recognition of the complementary nucleotides by **2** and **3** can be explained by strong competition of bulk water with possible hydrogen bonds between nucleobases. More intriguing is the observation that bis-adenine conjugate **3** showed the affinity toward poly U comparable to one observed for bis-uracil conjugate **2**, while in earlier studies we have observed that mono-adenine conjugate **6** formed significantly more stable complex with poly U than its uracil analogue **5** [10]. The steric hindrance of two adenines tethered to phenanthridinium and strong intramolecular interactions of **3** are the most probable causes of the failing selectivity.

Considering the *in vitro* biological activity assay, the most active of all studied compounds is the referent derivative **1**,

actually close structural analogue of ethidium bromide (**EB**). This structure proximity of **1** and **EB** was also reflected in poor selectivity toward cancer cell lines compared to a normal human fibroblast line. One order of magnitude lower activity of **4** pointed out that the absence of one amino group (compared to **1**) had a significant negative impact. Introduction of one nucleobase on to phenanthridinium system (**5–8**) yielded comparable activity toward cell lines as observed for **4** but in some cases had a significant impact on selectivity toward cancer cells compared to a normal human fibroblast. This selectivity was more pronounced for compounds with shorter linker between phenanthridinium and nucleobase (**5** and **6**). On the other hand, compound **7** having more flexible pentamethylene chain between phenanthridinium and uracil showed 2–3 times higher inhibitory activity against HeLa cell lines than its analogue **5** with shorter linker. A simple explanation and correlation of biological data with structure due to mode of activity is not possible owing to complexity of biological system. However, possible argument of observed selectivity could be steric hindrance of less flexible compound **5** being predominantly in folded conformation in water, which could partially hamper contact with the cell DNA. Bis-nucleobase conjugates **2** and **3** were found to be inactive, very likely due to a poor solubility in water under experimental conditions used.

None of the studied compounds is an intriguing candidate for the anticancer therapy. Nevertheless, systematic variation a) of number of substituents (one or two amino groups), b) variation of binding-active substituents (uracil, adenine) and c) flexibility of phenanthridinium–nucleobase system (linker length), has pointed out to measurable structure–biological activity correlation. Comparatively small structural changes in the simplest possible model of intercalator–nucleobase system have shown considerable impact not only on interactions with DNA and RNA but also on antiproliferative activity toward different cell lines and in some cases actually generated selectivity toward cancer cells compared with normal ones. This observation could be the starting point to the future research for more selective antitumour agents. Due to their selectivity toward specific polynucleotide sequences, as well as some selectivity against cancer cells compared to normal human fibroblast, compounds **5–8** are highly interesting candidates for examina-

tion of synergic effects in combination with currently available alkylating drugs that can produce multiple abasic lesions in the cell [8<sup>c</sup>]. Abasic site can be lethal if not repaired [27], thus compounds that are able to bind to specific abasic site can disassemble the lesion to the AP-endonuclease and therefore inhibit a repair process in damaged cell, so they have great potential as enhancers for anticancer therapy. Furthermore, future research in the field of model intercalator–nucleobase systems targeting specific polynucleotide sequences will be focused on the placement of recognition unit (nucleobase) into hydrophobic pocket between intercalator units.

## 5. Experimental

### 5.1. General procedures

<sup>1</sup>H NMR spectra were recorded on a Varian–Gemini 300 operating at 300 MHz, as well as on Bruker Avance DRX 500 operating at 500 MHz for <sup>1</sup>H. Chemical shifts ( $\delta$ ) are expressed in ppm, and  $J$  values in Hz. Signal multiplicities are denoted as s (singlet), d (doublet), t (triplet), q (quartet) and m (multiplet). The electronic absorption spectra were measured on a Varian Cary 100 Bio spectrometer. IR spectra were recorded on a Perkin–Elmer 297 instrument using KBr pellets. Fluorescence spectra were recorded on Perkin–Elmer LS 50 fluorimeter. Mass spectra were obtained using Extrel 2001 DD spectrometer. Preparative thin layer chromatography (TLC) was carried out using Kieselgel HF<sub>254</sub> “Merck”. Melting points were determined on Kofler apparatus and are uncorrected. 3,8-Bis-tosylamino-6-methylphenantridine was prepared starting from 4'-nitro-2-aminobiphenil, as previously described [28] For all products, purity was checked by <sup>1</sup>H NMR and for most of them correct elemental analyses were obtained. Only for **2** hygroscopic character of precipitate yielded elemental analyses with non-stoichiometric amounts of water; however, since NMR spectra of this compound were correct and **2** was obtained by simple chemical reactions from well characterised starting compounds, its structure is not questionable.

### 5.2. UV–vis and fluorescence measurements

Nucleotides and polynucleotides were purchased from Sigma and Aldrich, and used without further purification. Polynucleotide was dissolved in the sodium cacodylate buffer, 0.05 mol dm<sup>-3</sup>, pH = 7 and its concentration determined spectroscopically as the concentration of phosphates. The measurements were performed in aqueous buffer solution (pH = 5,  $I = 0.027$  mol dm<sup>-3</sup>, sodium citrate–HCl buffer). Under the experimental conditions used the absorbance and fluorescence intensities of **1–3** were proportional to their concentrations. Spectroscopic titrations were performed at constant ionic strength (buffer,  $I = 0.027$  mol dm<sup>-3</sup>) by adding portions of nucleotide or polynucleotide solution into solution of the tested compound. Obtained data were corrected for dilution. In fluorimetric titrations excitation wavelengths at  $\lambda_{\text{max}} > 440$  nm were used in order to avoid absorption of excitation light by added

nucleotides–polynucleotides and changes in emission at maxima (Table 1) were monitored. The binding constants and stoichiometries of complexes of **1–3** with the nucleotides were calculated for the concentration range corresponding to ca. 20–80% complexation by non-linear least-square fitting program SPECFIT [29].

### 5.3. Synthesis

#### 5.3.1. 3,8-Bis-(3-bromopropyltosyl)amino-6-methylphenantridine (**12**)

The 1,3-dibromopropane (5.7 ml, 56 mmol) and K<sub>2</sub>CO<sub>3</sub> (5.2 g, 38 mmol), were suspended in dry DMF (40 ml). To this suspension, solution of 3,8-bis-tosylamino-6-methylphenantridine (1 g, 1.88 mmol) in dry DMF (80 ml) was added dropwise during 30 min. and the reaction mixture was stirred during 48 hours under argon atmosphere at room temperature. Then, water and CH<sub>2</sub>Cl<sub>2</sub> were added to this suspension. Water layer was washed twice with CH<sub>2</sub>Cl<sub>2</sub>, organic extracts were dried over Na<sub>2</sub>SO<sub>4</sub> and evaporating. Water was added to brown oil to give light brown precipitate. Pure compound **12** was obtained by TLC (SiO<sub>2</sub>, 2% MeOH in CH<sub>2</sub>Cl<sub>2</sub>, R<sub>f</sub> = 0.46) as colourless oil (450 mg, 31%), that was crystallised from MeOH, white crystals: m.p. 157–160 °C; <sup>1</sup>H NMR (CDCl<sub>3</sub>)  $\delta$ : 2.02–2.14 (m, 2  $\times$  CH<sub>2</sub>, 4 H), 2.42 (s, Ts–CH<sub>3</sub>, 3 H), 2.45 (s, Ts–CH<sub>3</sub>, 3 H), 2.89 (s, Phen–CH<sub>3</sub>, 3 H), 3.46 (m, 2  $\times$  CH<sub>2</sub>Br, 4 H), 3.83 (m, 2  $\times$  NCH<sub>2</sub>, 4 H), 7.22–7.48 (m, 2  $\times$  Ts, 8H), 7.53 (d.d., Phen–H9, 1 H,  $J_1 = 8.72$  Hz,  $J_2 = 2.05$  Hz), 7.59–7.63 (m, Phen–H2, Phen–H4, 2 H), 7.88 (d, Phen–H7, 1 H,  $J = 1.79$  Hz), 8.48 (d, Phen–H1, 1 H,  $J = 8.46$  Hz), 8.55 (d, Phen–H10, 1 H,  $J = 8.71$  Hz) ppm; <sup>13</sup>C NMR (CDCl<sub>3</sub>) 21.34, 23.01, 29.64, 31.32, 31.5, 48.76, 49.05, 122.49, 122.97, 123.77, 126.32, 126.45, 127.03, 127.66, 127.77, 128.25, 129.61, 130.69, 131.38, 134.38, 138.56, 139.92, 143.87, 144.1, 159.43 ppm; IR (KBr)  $\nu$ : 2940, 2860, 1600, 1580, 1540, 1350, 1230, 1185, 1160, 1090, 945, 830, 810, 730, 710, 670 cm<sup>-1</sup>. Anal. Calcd for C<sub>34</sub>H<sub>35</sub>N<sub>3</sub>O<sub>4</sub>S<sub>2</sub>Br<sub>2</sub> (Mr = 773.60): C 52.79, H 4.56, N 5.43%; Found: C 52.74, H 4.69, N 5.38%.

#### 5.3.2. 3,8-Bis-(*n*-propyltosyl)amino-6-methylphenantridine (**13**)

Compound **13** was obtained as described for **12**; K<sub>2</sub>CO<sub>3</sub> (1.17 g, 8.47 mmol), 1-bromopropane (1 ml, 11.3 mmol) and 3,8-tosylamino-6-methylphenantridine (300 mg, 0.56 mmol) in dry DMF (3 + 5 ml) gave light brown oil, that was purified by TLC (SiO<sub>2</sub>, 2% MeOH in CH<sub>2</sub>Cl<sub>2</sub>, R<sub>f</sub> = 0.44) to afford colourless oil (192 mg, 55%), that was crystallised from MeOH/CH<sub>2</sub>Cl<sub>2</sub>, white powder: m.p. 79–83 °C; <sup>1</sup>H NMR (CDCl<sub>3</sub>)  $\delta$ : 0.93 (m, 2  $\times$  CH<sub>3</sub>, 6 H), 1.49 (m, 2  $\times$  CH<sub>2</sub>, 4 H), 2.41 (s, Ts–CH<sub>3</sub>, 3 H), 2.44 (s, Ts–CH<sub>3</sub>, 3 H), 2.87 (s, Phen–CH<sub>3</sub>, 3 H), 3.64 (m, 2  $\times$  NCH<sub>2</sub>, 4 H), 7.21–7.51 (m, 2  $\times$  Ts, Phen–H2, 9H), 7.59 (d, Phen–H4, 1 H,  $J_{2-4} = 1.93$  Hz), 7.63 (dd, Phen–H9, 1 H,  $J_{7-9} = 2.2$  Hz,  $J_{9-10} = 8.79$  Hz), 7.87, (d, Phen–H7, 1 H), 8.46 (d, Phen–H10, 1 H), 8.53 (d, Phen–H1, 1 H,  $J_{1-2} = 8.82$  Hz) ppm; <sup>13</sup>C NMR (CDCl<sub>3</sub>) 9.41, 9.64, 9.71, 39.9, 40.27, 110.42, 110.82,

111.69, 114.97, 115.64, 115.79, 117.6, 122.87 ppm; IR (KBr)  $\nu$ : 2960, 2940, 2880, 1650, 1610, 1600, 1580, 1570, 1480, 1350, 1210, 1170, 1070, 1030, 1010, 960, 890, 840, 810, 740, 730, 710, 670, 665, 640  $\text{cm}^{-1}$ ; Anal. Calcd for  $\text{C}_{34}\text{H}_{37}\text{N}_3\text{O}_4\text{S}_2$  (Mr = 615.79): C 66.31, H 6.06, N 6.82%; Found: C 66.18, H 5.87, N 7.07%.

### 5.3.3. 3,8-Bis-[3-(uracil-1-yl)propyltosyl]amino-6-methylphenantridine (**14**)

Uracil (217 mg, 1.94 mmol) that was previously dried, and NaH (77 mg, 60% w.w., 1.94 mmol), were suspended in dry DMF (5 ml) and stirred during 1 h in argon atmosphere at room temperature. To this suspension, solution of **12** (100 mg, 0.13 mmol) in dry DMF (10 ml) was added dropwise and the reaction mixture was stirred during 48 hours under argon atmosphere at 40–50 °C. Then, water and  $\text{CH}_2\text{Cl}_2$  were added to this suspension. Water layer was washed twice with  $\text{CH}_2\text{Cl}_2$ , organic extracts were dried over  $\text{Na}_2\text{SO}_4$  and evaporating. Water was added to brown oil to give light grey precipitate **14** (83 mg, 77%) that was filtered washed with water, and without further purification used in next step. Pure compound **14** was obtained by TLC ( $\text{SiO}_2$ , 10% MeOH in  $\text{CH}_2\text{Cl}_2$ ,  $R_f = 0.57$ ) as white solid, that was recrystallised from MeOH and small amount of water; m.p. 152–155 °C;  $^1\text{H}$  NMR (DMSO- $d_6$ )  $\delta$ : 1.7 (br,  $2 \times \text{CH}_2$ , 4 H), 2.4 (s, Ts- $\text{CH}_3$ , 3 H), 2.42 (s, Ts- $\text{CH}_3$ , 3 H), 2.8 (s, Phen- $\text{CH}_3$ , 3 H), 3.74 (m,  $2 \times \text{NCH}_2$ ,  $2 \times \text{CH}_2\text{Ura}$ , 8 H), 5.52 (m,  $2 \times \text{Ura-H5}$ , 2 H), 7.37–7.59 (m,  $2 \times \text{Ts}$ , Phen-H2, 9 H), 7.62 (m,  $2 \times \text{Ura-H6}$ , Phen-H9, 3 H), 7.71 (d, Phen-H4, 1 H,  $J_{2-4} = 1.87$  Hz), 7.88 (d, Phen-H7, 1 H,  $J_{7-9} = 1.87$  Hz), 8.73 (d, Phen-H1, 1 H,  $J_{1-2} = 9.03$  Hz), 8.82 (d, Phen-H10, 1 H,  $J_{9-10} = 9.02$  Hz), 11.21 (s,  $2 \times \text{Ura-NH}$ , 2 H) ppm;  $^{13}\text{C}$ -NMR (DMSO- $d_6$ )  $\delta$ : 21.18, 22.94, 27.35, 28.93, 38.77, 42.18, 49.88, 118.84, 122.87, 122.98, 124.0, 125.6, 125.96, 126.96, 127.66, 129.1, 129.31, 129.88, 131.21, 131.28, 134.47, 138.04, 140.93, 143.46, 143.87, 149.63, 152.44, 156.05, 158.3 ppm; IR (KBr)  $\nu$ : 3040, 2920, 1670, 1470, 1450, 1370, 1335, 1225, 1150, 1075, 940, 805, 760, 720, 700, 660, 645  $\text{cm}^{-1}$ ; Anal. Calcd for  $\text{C}_{42}\text{H}_{41}\text{N}_7\text{O}_8\text{S}_2 \times 3 \text{H}_2\text{O} \times \text{CH}_3\text{OH}$  (Mr = 889.98): C 56.68, H 5.32, N 11.01%; Found: C 56.84, H 5.2, N 10.57%; ES-MS ( $m/z$ ) calcd: 836.3 ( $\text{M}^+ + 1$ ), 418.6 ( $\text{M}^{2+} + 2$ ); found: 836.0 ( $\text{M}^+ + 1$ ), 418.7 ( $\text{M}^{2+} + 2$ ).

### 5.3.4. 3,8-Bis-[3-(aden-9-yl)propyltosyl]amino-6-methylphenantridine (**15**)

Compound **15** was obtained as described for **14**; adenine (270 mg, 1.94 mmol), NaH (77 mg, 60% w.w., 1.94 mmol) and **12** (100 mg, 0.13 mmol) in dry DMF (3 + 10 ml) gave white powder **15** (96 mg, 84%), that was without further purification used in next step. Pure compound **15** was obtained by TLC ( $\text{SiO}_2$ , 10% MeOH in  $\text{CH}_2\text{Cl}_2$ ,  $R_f = 0.26$ ) as white solid, that was recrystallised from MeOH; m.p. 185–188 °C;  $^1\text{H}$  NMR (DMSO- $d_6$ )  $\delta$ : 1.94 (br,  $2 \times \text{CH}_2$ , 4 H), 2.39 (s, Ts- $\text{CH}_3$ , 3 H), 2.41 (s, Ts- $\text{CH}_3$ , 3 H), 2.77 (s, Phen- $\text{CH}_3$ , 3 H), 3.75 (br,  $2 \times \text{NCH}_2$ , 4 H), 4.24 (m,  $2 \times \text{CH}_2\text{Ade}$ , 4 H), 7.3 (s,  $2 \times \text{NH}_2$ , 4 H), 7.37 (m,  $2 \times \text{Ts}$ , Phen-H2, 9 H), 7.64 (d,

Phen-H9, 1 H,  $J_{9-10} = 8.40$  Hz), 7.71 (s, Phen-H4, 1 H), 7.82 (s, Phen-H7, 1 H), 8.1 (m,  $2 \times \text{Ade-H2}$ ,  $2 \times \text{Ade-H8}$ , 4 H), 8.71 (d, Phen-H1, 1 H,  $J_{1-2} = 9.02$  Hz), 8.81 (d, Phen-H10, 1 H) ppm;  $^{13}\text{C}$  NMR (DMSO- $d_6$ )  $\delta$ : 21.08 (Ts- $\text{CH}_3$ ), 22.82 (Phen- $\text{CH}_3$ ), 27.99 ( $\text{CH}_2$ ), 47.64, 118.99, 122.95, 123.12, 124.22, 125.73, 126.45, 127.04, 127.81, 129.22, 129.44, 130.02, 131.25, 131.48, 134.33, 137.86, 141.18, 143.65, 144.15, 149.74, 152.6, 156.24, 158.48 ppm; IR (KBr)  $\nu$ : 3470, 3300, 3100, 2940, 1650, 1600, 1480, 1420, 1375, 1350, 1310, 1240, 1220, 1160, 1110, 1090, 1070, 1010, 950, 820, 800, 780, 730, 710, 670, 650  $\text{cm}^{-1}$ ; Anal. Calcd for  $\text{C}_{44}\text{H}_{43}\text{N}_{13}\text{O}_4\text{S}_4$  (Mr = 881.30): C 59.91, H 4.92, N 20.66%; Found: C 59.74, H 5.17, N 20.57%.

### 5.3.5. 3,8-Bis(propyl)amino-6-methylphenantridine (**1**)

Compound **13** (100 mg, 0.16 mmol) was dissolved in 5 ml conc.  $\text{H}_2\text{SO}_4$  and heated under reflux at 80–100 °C for 2 h. Reaction mixture was cooled, poured on ice and made alkaline (pH = 8–9) by addition of 2 M NaOH. Red solid **1** (74 mg, 78%) was precipitated, filtered and washed with a lots of water, then purified by TLC ( $\text{SiO}_2$ , 10% MeOH in  $\text{CH}_2\text{Cl}_2$ ,  $R_f = 0.65$ ) and finally recrystallised from MeOH and small amount of water; m.p. 118–121 °C;  $^1\text{H}$  NMR (DMSO- $d_6$ )  $\delta$ : 0.98 (m,  $2 \times \text{CH}_3$ , 6 H), 1.61 (m,  $2 \times \text{CH}_2$ , 4 H), 2.75 (s, Phen- $\text{CH}_3$ , 3 H), 3.07 (m,  $2 \times \text{NCH}_2$ , 4 H), 5.85 (br, NH, 1 H), 5.97 (br, NH, 1 H), 6.82 (s, Phen-H4, 1 H), 6.90–6.93 (m, Phen-H7, Phen-H2, 2 H), 7.17 (d, Phen-H9, 1 H,  $J = 8.97$  Hz), 8.14 (d, Phen-H1, 1 H,  $J = 8.97$  Hz), 8.24 (d, Phen-H10, 1 H,  $J = 8.98$  Hz) ppm;  $^{13}\text{C}$  NMR (DMSO- $d_6$ )  $\delta$ : 11.9, 11.97, 23.15, 44.88, 103.08, 106.11, 115.92, 120.11, 121.79, 122.3, 123.77, 125.31, 143.5, 146.79, 147.95, 156.82 ppm; IR (KBr)  $\nu$ : 3420, 3280, 2960, 2930, 2880, 1620, 1580, 1510, 1475, 1430, 1390, 1365, 1250, 1220, 1180, 1150, 1075, 1010, 950, 830, 810, 720, 670  $\text{cm}^{-1}$ ; Anal. Calcd for  $\text{C}_{20}\text{H}_{25}\text{N}_3$  (Mr = 307.44): C 78.14, H 8.20, N 13.67%; Found: C 78.41, H 7.98, N 13.56%.

### 5.3.6. 3,8-Bis-[3-(uracil-1-yl)propyl]amino-6-methylphenantridine (**2**)

Compound **2** (150 mg, 0.18 mmol) was obtained as described for **1**; **14** in mixture of 1 ml conc.  $\text{H}_2\text{SO}_4$  and 2 ml conc. acetic acid, gave red solid **2** (74 mg, 78%) that was purified by TLC ( $\text{SiO}_2$ , 20% MeOH in  $\text{CH}_2\text{Cl}_2$ ,  $R_f = 0.45$ ) and finally recrystallised from MeOH and  $\text{H}_2\text{O}$ ; yellow powder; m.p. 129–134 °C;  $^1\text{H}$  NMR (DMSO- $d_6$ )  $\delta$ : 1.96 (br,  $2 \times \text{CH}_2$ , 4 H), 2.85 (s, Phen- $\text{CH}_3$ , 3 H), 3.18 (br,  $2 \times \text{NCH}_2$ , 4 H), 3.83 (t,  $2 \times \text{CH}_2\text{Ura}$ , 4 H,  $J = 6.84$  Hz), 5.57 (d,  $2 \times \text{Ura-H5}$ , 2 H,  $J = 7.16$  Hz), 6.18 (s,  $2 \times \text{NH}$ , 2 H), 6.91 (s, Phen-H4, 1 H), 6.99–7.02 (m, Phen-H7, Phen-H2, 2 H), 7.27 (d, Phen-H9, 1 H,  $J = 9.03$  Hz), 7.71 (d,  $2 \times \text{Ura-H6}$ , 2 H,  $J = 7.78$  Hz), 8.26 (d, Phen-H1, 1 H,  $J = 9.03$  Hz), 8.34 (d, Phen-H10, 1 H,  $J = 9.03$  Hz), 11.29 (s,  $2 \times \text{Ura-NH}$ , 2 H) ppm; IR (KBr)  $\nu$ : 3350, 2920, 1660, 1610, 1570, 1505, 1450, 1340, 1330, 1280, 1230, 1170, 1150, 1050, 800, 750, 705  $\text{cm}^{-1}$ ; ES-MS ( $m/z$ ) 528.2 ( $\text{M}^+ + 1$ ), 264.6 ( $\text{M}^{2+} + 2$ ); found: 528.1 ( $\text{M}^+ + 1$ ), 264.7 ( $\text{M}^{2+} + 2$ ).

### 5.3.7. 3,8-Bis[3-(aden-9-yl)propyl]amino-6-methylphenantridine (3)

Compound **3** was obtained as described for **1**; **15** (90 mg, 0.1 mmol) in 1 ml conc. H<sub>2</sub>SO<sub>4</sub> and 3 ml conc. acetic acid gave yellow powder (50 mg, 84%) **3**, that was purified by TLC (SiO<sub>2</sub>, 20% MeOH in CH<sub>2</sub>Cl<sub>2</sub>, R<sub>f</sub> = 0.08) and recrystallised from MeOH and small amount of water; m.p. >300 °C; <sup>1</sup>H NMR (DMSO-d<sub>6</sub>) 2.28 (br, 2 × CH<sub>2</sub>, 4 H), 2.84 (s, Phen-CH<sub>3</sub>, 3 H), 3.27 (m, 2 × NCH<sub>2</sub>, 4 H), 4.42 (br, 2 × CH<sub>2</sub>Ade, 4 H, *J* = 6.84 Hz), 6.12 (br, NH, 1 H), 6.26 (br, NH, 1 H), 6.97 (s, Phen-H4, 1 H), 7.03–7.07 (m, Phen-H7, Phen-H2, 2 H), 7.31 (m, Phen-H9, NH<sub>2</sub>, 3 H), 8.27 and 8.30 (s, 2 × Ade-H2, 2 × Ade-H8, 4 H), 8.43 (m, Phen-H1, Phen-H10, 2 H) ppm; IR (KBr) ν: 3300, 3100, 2910, 2840, 1650, 1600, 1570, 1505, 1460, 1405, 1380, 1330, 1300, 1240, 1190, 1155, 1000, 800, 710, 640 cm<sup>-1</sup>; Anal. Calcd for C<sub>30</sub>H<sub>31</sub>N<sub>13</sub> × 2 H<sub>2</sub>O × CH<sub>3</sub>OH (Mr = 641.75): C 58.01, H 6.12, N 28.37%; Found: C 57.74, H 5.77, N 28.0%; ES-MS (*m/z*) calcd: 574.3 (M<sup>+</sup> + 1), 287.6 (M<sup>2+</sup> + 2), 192.1 (M<sup>2+</sup> + 3); found: 574.0 (M<sup>+</sup> + 1), 287.7 (M<sup>2+</sup> + 2), 192.2 (M<sup>2+</sup> + 3).

### 5.4. Molecular modelling, molecular mechanics, molecular dynamics and semiempirical study

Semiempirical calculations were performed with the program MOPAC, using AM1 calculations. The geometry optimisation of a molecule was performed in two steps: a) with the all heavy atoms fixed, b) with all atoms free to move.

Force field calculations were performed using the all-atom AMBER force field [20], and the partial atomic charges derived from the electrostatic potential fitted AM1 calculations. Energy minimization was performed by the steepest descent and conjugate gradients algorithms. Systems were optimised up to the convergence of about 0.01 kcal mol<sup>-1</sup>. The molecular dynamic simulation was accomplished using the time step of 1 fs and the Varlet integration method. MD simulations with the explicit water molecules were performed using PBC with the cubic unit cell dimensions 31 × 31 × 31 Å. NVT assemble was used and the cut-off distances of 13 and 15 Å. System was equilibrated for 3000 steps and then the temperature was slowly increasing 50 K/1000 steps up to 300 K. At room temperature simulation was performed in duration of about 1 ns.

### 5.5. Antitumour activity assays

The growth inhibition activity was assessed according to the slightly modified procedure performed at the National Cancer Institute, Developmental Therapeutics Program [30]. The HeLa (cervical carcinoma), MCF-7 (breast carcinoma), SW 620 (colon carcinoma), MiaPaCa-2 (pancreatic carcinoma), Hep-2 (laryngeal carcinoma) and WI 38 (diploid fibroblasts) cells were cultured as monolayers and maintained in Dulbecco's modified Eagle's medium (DMEM) supplemented with 10% fetal bovine serum (FBS), 2 mM L-glutamine, 100 U ml<sup>-1</sup> penicillin and 100 μg ml<sup>-1</sup> streptomycin in a humidified atmosphere with 5% CO<sub>2</sub> at 37 °C. The cells were inoculated onto

standard 96-well microtiter plates on day 0. The cell concentrations were adjusted according to the cell population doubling time (PDT): 1 × 10<sup>4</sup> per ml for HeLa, Hep-2, MiaPaCa-2 and SW 620 cell lines (PDT = 20–24 hours) 2 × 10<sup>4</sup> per ml for MCF-7 cell lines (PDT = 33 hours) and 3 × 10<sup>4</sup> per ml for WI 38 (PDT = 47 hours). Test agents were then added in five, 10-fold dilutions (10<sup>-8</sup>–10<sup>-4</sup> mol dm<sup>-3</sup>) and incubated for further 72 hours. Working dilutions were freshly prepared on the day of testing. The solvent was also tested for eventual inhibitory activity by adjusting its concentration to be the same as in working concentrations. After 72 hours of incubation, the cell growth rate was evaluated by performing the MTT assay [31], which detects dehydrogenase activity in viable cells. The absorbency (OD, optical density) was measured on a microplate reader at 570 nm. The percentage of growth (PG) of the cell lines was calculated according to one or the other of the following two expressions:

If (mean OD<sub>test</sub> – mean OD<sub>tzero</sub>) ≥ 0 then

$$PG = 100 \times (\text{mean OD}_{\text{test}} - \text{mean OD}_{\text{tzero}}) / (\text{mean OD}_{\text{ctrl}} - \text{mean OD}_{\text{tzero}}).$$

If (mean OD<sub>test</sub> – mean OD<sub>tzero</sub>) < 0 then:

$$PG = 100 \times (\text{mean OD}_{\text{test}} - \text{mean OD}_{\text{tzero}}) / \text{OD}_{\text{tzero}}.$$

Where:

Mean OD<sub>tzero</sub> = the average of optical density measurements before exposure of cells to the test compound.

Mean OD<sub>test</sub> = the average of optical density measurements after the desired period of time.

Mean OD<sub>ctrl</sub> = the average of optical density measurements after the desired period of time with no exposure of cells to the test compound.

Each test point was performed in quadruplicate three individual experiments. The results are expressed as IC<sub>50</sub>, which is the concentration necessary for 50% of inhibition. The IC<sub>50</sub> values for each compound are calculated from dose–response curves using linear regression analysis by fitting the test concentrations that give PG values above and below the reference value (i.e. 50%). If however, for a given cell line all of the tested concentrations produce PGs exceeding the respective reference level of effect (e.g. PG value of 50), then the highest tested concentration is assigned as the default value, which is preceded by a “>” sign.

### Acknowledgments

Support for this study by the Ministry of Science, Education and Sport of Croatia is gratefully acknowledged (Projects 0098053, 0119641, 0098093, 0098036)

### References

- [1] S. Yoshizawa, G. Kawai, K.A. Watanabe, K.I. Miura, I. Hirao, *Biochemistry* 36 (1997) 4761–4767.
- [2] H. Naegeli, *Mechanism of DNA Damage Recognition in Mammalian Cells*, R.G. Landes Company, Austin, Texas, USA, Springer-Verlag, Heidelberg, Germany, 1997.
- [3] C. Bailly, M.J. Waring, in: K.R. Fox (Ed.), *Methods in Molecular Biology*, Humana Press, Totowa, NJ, 1997, pp. 51–79 (vol. 90).

- [4] J.-C. François, N.T. Thuong, C. Hélène, *Nucleic Acids Res.* 22 (1994) 3943–3950.
- [5] P.T. Henderson, B. Armitage, G.B. Schuster, *Biochemistry* 37 (1998) 2991–3000.
- [6] G. Juan, W. Pan, M. Darzynkiewicz, *Exp. Cell Res.* 227 (1996) 197–202.
- [7] K. Hemminki, D.B.J. Ludlum, *Natl. Cancer Inst.* 73 (1984) 1021–1028.
- [8] a) Y. Coppel, J.-F. Constant, C. Coulombeau, M. Demeunynck, J. Garcia, J. Lhomme, *Biochemistry* 36 (1997) 4831–4843; b) P. Belmont, M. Jourdan, M. Demeunynck, J.-F. Constant, J. Garcia, J. Lhomme, D. Carrez, A. Croisy, *J. Med. Chem.* 42 (1999) 5153–5159; c) J. Lhomme, J.-F. Constant, M. Demeunynck, *Biopolymers* 52 (1999) 65–83; d) J. M. Barret, C. Etievant, J. Fahy, J. Lhomme, B.T. Hill, *Anticancer Drugs* 10 (1999) 55–65; e) K. Alarcon, M. Demeunynck, J. Lhomme, D. Carrez, A. Croisy, *Bioorg. Med. Chem.* 9 (2001) 1901–1910; f) A. Martelli, J.F. Constant, M. Demeunynck, J. Lhomme, P. Dumy, *Tetrahedron* 58 (2002) 4291–4298.
- [9] L.-M. Tumir, I. Piantanida, P. Novak, M. Žinić, *J. Phys. Org. Chem.* 15 (2002) 599–607.
- [10] I. Juranović, Z. Meić, I. Piantanida, L.-M. Tumir, M. Žinić, *Chem. Commun.* (2002) 1432–1433.
- [11] L.-M. Tumir, I. Piantanida, I. Juranović Cindrić, T. Hrenar, Z. Meić, M. Žinić, *J. Phys. Org. Chem.* 16 (2003) 891–899.
- [12] L.-M. Tumir, I. Piantanida, I. Juranović, Z. Meić, S. Tomić, M. Žinić, *Chem. Commun.* (2005) 2561–2563.
- [13] S. Takenaka, M. Manabe, M. Yokoyama, M. Nishi, J. Tanaka, H. Kondo, *Chem. Commun.* (1996) 379–380.
- [14] I. Piantanida, B.S. Palm, P. Čudić, M. Žinić, H.-J. Schneider, *Tetrahedron Lett.* 42 (2001) 6779–6783.
- [15] a) N. Berthet, J. Michon, J. Lhomme, M.P. Teulade-Fichou, J.P. Vigneron, J.-M. Lehn, *Chem. Eur. J.* 5 (1999) 3625–3630; b) M. Jourdan, J. Garcia, J. Lhomme, M.P. Teulade-Fichou, J.P. Vigneron, J.-M. Lehn, *Biochemistry* 38 (43) (1999) 14205–14213.
- [16] a) D. M. Crothers, *Biopolymers*, 6 (1968) 575–584.; b) J.L. Botour, E. Delain, D. Coulaud, J.B. LePecq, J. Barbet, B. P, Roques, *Biopolymers* 17 (1978) 872–886.
- [17] N.J. Leonard, R.F. Lambert, *J. Org. Chem.* 34 (1969) 3240–3248.
- [18] DNA and RNA binders, in: M. Demeunynck, C. Bailly, W.D. Wilson (Eds.), Wiley-VCH, Weinheim, 2002.
- [19] J.-L. Dimicoli, C. Hélène, *J. Am. Chem. Soc.* 95 (1974) 1036–1044.
- [20] W.D. Cornell, P. Cieplak, C.I. Payly, I.R. Gould, K.M. Merz, D.M. Ferguson, D.C. Spellmeyer, T. Fox, J.W. Caldwell, P.A. Kollman, *J. Am. Chem. Soc.* 117 (1995) 5179–5197.
- [21] I. Piantanida, V. Tomišić, M. Žinić, *J. Chem. Soc. Perkin Trans. 2* (2000) 375–383.
- [22] A. Odani, H. Masuda, O. Yamauchi, S. Ishiguro, *Inorg. Chem.* 30 (1991) 4486–4488.
- [23] N.W. Luedtke, Dissertation, University of California, San Diego, 2002.
- [24] S. Georghiou, *Photochem. Photobiol.* 26 (1977) 59–68.
- [25] M.-P. Teulade, J.-M. Lehn, J.-P. Vigneron, *J. Supramol. Chem.* 5 (1995) 139–147.
- [26] I. Piantanida, B.S. Palm, M. Žinić, H.-J. Schneider, *J. Chem. Soc. Perkin Trans. 2* (2001) 1808–1816.
- [27] A. Gentil, G. Renault, C. Madzak, A. Margot, J.B. Cabral-Neto, J.J. Vas-seur, B. Rayner, J.L. Imbach, A. Sarasin, *Biochem. Biophys. Res. Commun.* 173 (1990) 704–710.
- [28] a) J. Cymerman, W.F. Short, *J. Org. Chem.* (1949) 703–704; b) J.W. Lown, B.C. Gunn, K.C. Majumdar, E. McGoran, *Can. J. Chem.* 57 (1979) 2305–2313.
- [29] a) S P E C F I T G L O B A L A N A L Y S I S, a Program for Fitting, Equilibrium and Kinetic Systems, using Factor Analysis & Marquardt Minimization; b) H. Gampp, M. Maeder, C.J. Meyer, A.D. Zuberbuehler, *Talanta* 32 (1985) 257–264; c) M. Maeder A.D. Zuberbuehler, *Anal. Chem.* 62 (1990) 2220–2224.
- [30] M.R. Boyd, K.D. Paull, *Drug Dev. Res.* 34 (1995) 91–109.
- [31] T. Mossman, *J. Immunol. Methods* 65 (1983) 55–63.